

MSSM Higgs-boson production in bottom-quark fusion: electroweak radiative corrections

STEFAN DITTMAIER

*Max-Planck-Institut für Physik (Werner-Heisenberg-Institut),
D-80805 München, Germany*

MICHAEL KRÄMER, ALEXANDER MÜCK

*Institut für Theoretische Physik E, RWTH Aachen,
D-52056 Aachen, Germany*

TOBIAS SCHLÜTER

*Max-Planck-Institut für Physik (Werner-Heisenberg-Institut),
D-80805 München, Germany*

Abstract:

Higgs-boson production in association with bottom quarks is an important discovery channel for supersymmetric Higgs particles at hadron colliders for large values of $\tan\beta$. We present the complete $\mathcal{O}(\alpha)$ electroweak and $\mathcal{O}(\alpha_s)$ strong corrections to associated bottom–Higgs production through $b\bar{b}$ fusion in the MSSM and improve this next-to-leading-order prediction by known two-loop contributions to the Higgs self-energies, as provided by the program `FeynHiggs`. Choosing proper renormalization and input-parameter schemes, the bulk of the corrections (in particular the leading terms for large $\tan\beta$) can be absorbed into an improved Born approximation. The remaining non-universal corrections are typically of the order of a few per cent. Numerical results are discussed for the benchmark scenarios SPS 1b and SPS 4.

March 2007

1 Introduction

The Higgs mechanism is a cornerstone of the Standard Model (SM) and its supersymmetric extensions. The masses of the fundamental particles, electroweak gauge bosons, leptons, and quarks, are generated by interactions with Higgs fields. The search for Higgs bosons is thus one of the most important endeavours in high-energy physics and is being pursued at the upgraded proton–antiproton collider Tevatron with a centre-of-mass (CM) energy of 1.96 TeV, followed in the near future by the proton–proton collider LHC with 14 TeV CM energy.

Various channels can be exploited to search for Higgs bosons at hadron colliders. Higgs radiation off bottom quarks [1]

$$p\bar{p}/pp \rightarrow b\bar{b}\phi^0 + X \quad (1.1)$$

is the dominant Higgs-boson production mechanism in supersymmetric theories at large $\tan\beta$, where the bottom–Higgs Yukawa couplings are, in general, strongly enhanced. With $\phi^0 = H, h^0, H^0, A^0$ we denote the SM Higgs boson or any of the neutral Higgs bosons of the Minimal Supersymmetric Standard Model (MSSM). Current searches for MSSM bottom–Higgs associated production at the Fermilab Tevatron widely exclude values $\tan\beta \gtrsim 50$ for light $M_{A^0} \approx 100$ GeV [2,3], depending in detail on the value of the Higgs mixing parameter μ .

Two different formalisms have been employed to calculate the cross section for associated $b\bar{b}\phi^0$ production. In a four-flavour number scheme (4FNS) with no b quarks in the initial state, the lowest-order QCD production processes are gluon–gluon fusion and quark–antiquark annihilation, $gg \rightarrow b\bar{b}\phi^0$ and $q\bar{q} \rightarrow b\bar{b}\phi^0$, respectively. The inclusive cross section for $gg \rightarrow b\bar{b}\phi^0$ develops large logarithms $\sim \ln(\mu_F/m_b)$, which arise from the splitting of gluons into nearly collinear $b\bar{b}$ pairs. The large scale $\mu_F \sim M_{\phi^0}$ corresponds to the upper limit of the collinear region up to which factorization is valid. The $\ln(\mu_F/m_b)$ terms can be summed to all orders in perturbation theory by introducing bottom parton densities. This defines the so-called five-flavour number scheme (5FNS) [4]. The use of bottom distribution functions is based on the approximation that the outgoing b quarks are at small transverse momentum. In this scheme, the leading-order (LO) process for the inclusive $b\bar{b}\phi^0$ cross section is $b\bar{b}$ fusion,

$$b\bar{b} \rightarrow \phi^0. \quad (1.2)$$

The next-to-leading order (NLO) cross section in the 5FNS includes $\mathcal{O}(\alpha_s)$ corrections to $b\bar{b} \rightarrow \phi^0$ and the tree-level processes $gb \rightarrow b\phi^0$ and $g\bar{b} \rightarrow \bar{b}\phi^0$.

To all orders in perturbation theory the four- and five-flavour schemes are identical, but the way of ordering the perturbative expansion is different, and the results do not match exactly at finite order. However, numerical comparisons between calculations of inclusive Higgs production in the two schemes [5–8] show that the two approaches agree within their respective uncertainties, once higher-order QCD corrections are taken into account.

There has been considerable progress recently in improving the cross-section predictions for inclusive associated $b\bar{b}\phi^0$ production by calculating NLO-QCD [5,7] and SUSY-QCD [9] corrections in the four-flavour scheme, and NNLO QCD corrections [10,11] in the five-flavour scheme. The inclusion of higher-order effects is crucial for an accurate theoretical prediction and, eventually, a determination of Higgs-boson parameters from the comparison of theory and experiment. In this paper we further improve the cross-section prediction and present the first calculation of the complete $\mathcal{O}(\alpha)$ electroweak corrections to associated bottom–Higgs production through $b\bar{b} \rightarrow \phi^0$ in the MSSM.

The complete one-loop QCD and electroweak corrections for the decay of MSSM Higgs bosons to bottom quarks have been presented in Ref. [12] more than a decade ago. While the predictions

for Higgs-boson decays have been improved and refined in recent years, supersymmetric QCD and electroweak corrections to the production cross section have so far only been investigated at the level of universal corrections for large $\tan\beta$ (see e.g. Refs. [3, 13]).

In Section 2.1 we shall set the notation for the supersymmetric model. The calculation of the NLO QCD and electroweak corrections is described in some detail in Sections 2.2, 2.3, and 2.4. Numerical results for MSSM Higgs-boson production at the LHC are presented in Section 3. We conclude in Section 4. The Appendices provide details on the scenarios of the supersymmetric model under consideration and present further numerical results.

2 Radiative corrections

2.1 Tree-level Yukawa couplings and cross section

In the Standard Model, Higgs production from bottom-quark fusion is governed by the interaction term

$$\mathcal{L}_{\bar{b}bH} = -\lambda_b^{\text{SM}} \bar{b} b H, \quad (2.1)$$

where λ_b is the bottom-quark Yukawa coupling and H denotes the field of the physical Higgs boson. The corresponding mass term for the bottom quark is generated by the Higgs vacuum expectation value v , leading to the tree-level relation

$$\lambda_b^{\text{SM}} = \frac{m_b}{v} = \frac{e m_b}{2s_w M_W}, \quad (2.2)$$

where e is the electromagnetic coupling constant, s_w the sine of the weak mixing angle, and M_W the W-boson mass.

For the MSSM we will follow the conventions of Ref. [14], where the two Higgs doublets are denoted as

$$H_d = \begin{pmatrix} h_d^+ \\ \frac{1}{\sqrt{2}}(v_d + h_d^0 + i\chi_d^0) \end{pmatrix}, \quad H_u = \begin{pmatrix} \frac{1}{\sqrt{2}}(v_u + h_u^0 - i\chi_u^0) \\ -h_u^- \end{pmatrix}. \quad (2.3)$$

The bottom quarks couple to H_d , giving mass to the down-type quarks via the vacuum expectation value v_d . Masses for up-type quarks are generated by a second Higgs doublet H_u with vacuum expectation value v_u . Considering the MSSM without CP-violating phases, the CP-even neutral Higgs-boson fields h^0 and H^0 are linear combinations of h_d^0 and h_u^0 . One conventionally defines the Higgs mixing angle α by writing

$$\begin{pmatrix} h^0 \\ H^0 \end{pmatrix} = \begin{pmatrix} c_\alpha & -s_\alpha \\ s_\alpha & c_\alpha \end{pmatrix} \begin{pmatrix} h_u^0 \\ h_d^0 \end{pmatrix}. \quad (2.4)$$

Here and in the following, we will frequently use the notation $s_\alpha \equiv \sin\alpha$, $c_\alpha \equiv \cos\alpha$ and generalizations thereof. The vacuum expectation values are parameterized according to $v_u = v \sin\beta$, $v_d = v \cos\beta$, i.e.

$$t_\beta \equiv \tan\beta \equiv \frac{v_u}{v_d} \quad \text{and} \quad v^2 \equiv v_u^2 + v_d^2. \quad (2.5)$$

Taking the pseudoscalar Higgs mass M_{A^0} and t_β as input parameters of the MSSM Higgs sector, one finds the tree-level relation

$$t_{2\alpha} = \frac{M_{A^0}^2 + M_Z^2}{M_{A^0}^2 - M_Z^2} t_{2\beta} \quad (2.6)$$

with $s_{2\alpha} < 0$. The fields of the physical neutral pseudoscalar Higgs boson A^0 and the neutral would-be Goldstone boson G^0 are given by

$$\begin{pmatrix} A^0 \\ G^0 \end{pmatrix} = \begin{pmatrix} c_\beta & -s_\beta \\ s_\beta & c_\beta \end{pmatrix} \begin{pmatrix} \chi_u^0 \\ \chi_d^0 \end{pmatrix}. \quad (2.7)$$

Consequently, the $b\bar{b}h^0$, $b\bar{b}H^0$, and $b\bar{b}A^0$ couplings read

$$\begin{aligned} \lambda_b^{h^0} &= \frac{-s_\alpha m_b}{v_d} = -\lambda_b^{\text{SM}} \frac{s_\alpha}{c_\beta}, \\ \lambda_b^{H^0} &= \frac{c_\alpha m_b}{v_d} = \lambda_b^{\text{SM}} \frac{c_\alpha}{c_\beta}, \\ \lambda_b^{A^0} &= \frac{-s_\beta m_b}{v_d} = -\lambda_b^{\text{SM}} t_\beta. \end{aligned} \quad (2.8)$$

Hence, the Yukawa couplings are enhanced for large values of t_β . Note that for large masses of the pseudoscalar Higgs boson, h^0 is known to be SM like and $s_\alpha \rightarrow -c_\beta$.

The leading-order partonic cross sections are given by

$$\hat{\sigma}_{\phi^0}^0 = \frac{\pi}{6} \frac{(\lambda_b^{\text{SM}})^2}{M_{\phi^0}^2} \delta(1 - \tau) \begin{cases} s_\alpha^2/c_\beta^2 & h^0 \\ c_\alpha^2/c_\beta^2 & \text{for } H^0 \text{ production,} \\ t_\beta^2 & A^0 \end{cases} \quad (2.9)$$

where $\phi^0 = (h^0, H^0, A^0)$, $\tau = M_{\phi^0}^2/\hat{s}$, $\sqrt{\hat{s}}$ is the partonic CM energy, and the incoming bottom quarks are treated as massless particles in accordance with QCD factorization.

2.2 SUSY-QCD corrections

The QCD corrections to the process $b\bar{b} \rightarrow h^0, H^0, A^0$ are known to NNLO [10, 11], with a small residual QCD factorization and renormalization scale uncertainty of less than $\sim 10\%$. If one chooses the renormalization and factorization scales as $\mu_R = M_H$ and $\mu_F = M_H/4$, respectively, the impact of the genuine NNLO QCD corrections is typically less than 5% [11]. We have reproduced the NLO QCD result and extend previous analyses by including the $\mathcal{O}(\alpha_s)$ SUSY-QCD corrections from virtual squark and gluino exchange.

The $\overline{\text{MS}}$ scheme has been adopted for the renormalization of the bottom-quark mass m_b and for the factorization of initial-state collinear singularities. The renormalization of the bottom-Higgs Yukawa coupling is fixed in terms of the bottom-mass renormalization. In order to sum large logarithmic corrections $\propto \ln(m_b/\mu_R)$ we evaluate the Yukawa coupling with the running b-quark mass $\overline{m}_b(\mu_R)$ [15].

The $\mathcal{O}(\alpha_s)$ SUSY-QCD corrections comprise self-energy and vertex diagrams induced by virtual sbottom and gluino exchange, as shown in Fig. 1. It is well known [16–19] that the SUSY-QCD corrections are enhanced for large t_β . This important effect can be qualitatively understood as follows. Unlike down-type quarks, which only couple to the down-type Higgs field at tree level, the down-type squarks also couple to the up-type Higgs field via terms in the superpotential. The corresponding coupling strength is proportional to the enhanced Yukawa coupling m_b/v_d times the Higgs mixing parameter μ . Hence, the vacuum expectation value v_u of H_u leads to a mixing term in the sbottom mass matrix proportional to μt_β , which dominates the sbottom mixing angle $\Theta_{\tilde{b}}$,

$$\sin(2\Theta_{\tilde{b}}) = \frac{2m_b (A_b - \mu t_\beta)}{m_{\tilde{b}_1}^2 - m_{\tilde{b}_2}^2}, \quad (2.10)$$

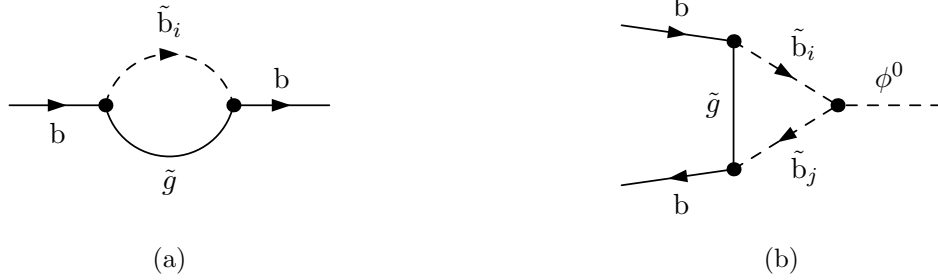


Figure 1: Self-energy (a) and vertex (b) corrections from gluino exchange. Sbottom mass eigenstates are denoted as \tilde{b}_i with $i = 1, 2$.

where A_b denotes the soft-supersymmetry-breaking trilinear scalar coupling and $\tilde{b}_{1,2}$ are the sbottom mass eigenstates. The factor $\sin(2\Theta_{\tilde{b}})$ directly enters the (scalar part of the) b-quark self-energy, which in turn enters the Yukawa coupling renormalization via the b-mass counterterm δm_b . The corresponding mass shift is usually denoted by $-m_b \Delta_b$ with

$$\Delta_b = \frac{C_F \alpha_s}{2} \frac{m_{\tilde{g}}}{\pi} \mu t_\beta I(m_{\tilde{b}_1}, m_{\tilde{b}_2}, m_{\tilde{g}}), \quad (2.11)$$

$C_F = 4/3$, and the auxiliary function

$$I(a, b, c) = \frac{-1}{(a^2 - b^2)(b^2 - c^2)(c^2 - a^2)} \left(a^2 b^2 \ln \frac{a^2}{b^2} + b^2 c^2 \ln \frac{b^2}{c^2} + c^2 a^2 \ln \frac{c^2}{a^2} \right). \quad (2.12)$$

Here, $m_{\tilde{g}}$ is the gluino mass. As shown in Ref. [20] by power counting in $\alpha_s t_\beta$, the contribution of Δ_b can be summed by the replacement

$$m_b \rightarrow \frac{m_b}{1 + \Delta_b} \quad (2.13)$$

in the bottom Yukawa coupling. As explained above, the loop-induced coupling of the up-type Higgs to bottom quarks also involves a factor $\alpha_s t_\beta$. The full contribution to the $\phi^0 b \bar{b}$ vertex receives an additional factor $\{c_\alpha, s_\alpha, c_\beta\}$ from the H_u part in $\phi^0 = \{h^0, H^0, A^0\}$. Power counting in $\alpha_s t_\beta$ shows [20] that the t_β -enhanced vertex corrections of the form $(\alpha_s t_\beta)^n$ are one-loop exact, i.e. they do not appear at higher orders ($n \geq 2$). Collecting all t_β -enhanced corrections to the bottom Yukawa couplings leads to the effective couplings $\bar{\lambda}_b^{\phi^0}$ [20, 21], where

$$\begin{aligned} \frac{\bar{\lambda}_b^{h^0}}{\lambda_b^{\text{SM}}} &= -\frac{s_\alpha}{c_\beta} \frac{1 - \Delta_b/(t_\beta t_\alpha)}{1 + \Delta_b}, \\ \frac{\bar{\lambda}_b^{H^0}}{\lambda_b^{\text{SM}}} &= \frac{c_\alpha}{c_\beta} \frac{1 + \Delta_b t_\alpha/t_\beta}{1 + \Delta_b}, \\ \frac{\bar{\lambda}_b^{A^0}}{\lambda_b^{\text{SM}}} &= -t_\beta \frac{1 - \Delta_b/t_\beta^2}{1 + \Delta_b}. \end{aligned} \quad (2.14)$$

Note that $\bar{\lambda}_b^{h^0}$ is still SM like for large M_{A^0} , independent of the large- t_β summation owing to $t_\beta t_\alpha \rightarrow -1$ in this limit. The summation formalism can be extended [21] to include corrections

proportional to the trilinear coupling A_b in (2.10). However, these corrections turn out to be small and summation effects may thus safely be neglected for the MSSM scenarios under consideration in this work.

To combine the features of the above effective treatment with the complete one-loop SUSY-QCD calculation, we modify the renormalization scheme to absorb the above corrections into a redefinition of the bottom mass in the Yukawa coupling. Hence, an additional counterterm

$$\frac{\bar{\delta}m_b^{h^0}}{m_b} = \Delta_b \left(1 + \frac{1}{t_\alpha t_\beta}\right), \quad \frac{\bar{\delta}m_b^{H^0}}{m_b} = \Delta_b \left(1 - \frac{t_\alpha}{t_\beta}\right), \quad \frac{\bar{\delta}m_b^{A^0}}{m_b} = \Delta_b \left(1 + \frac{1}{t_\beta^2}\right) \quad (2.15)$$

is added for h^0 , H^0 , and A^0 production, respectively, to remove the t_β -enhanced contributions from the explicit one-loop result in order to avoid double-counting. We use the convention of Ref. [12] where $m_{b,0} = m_b + \delta m_b$.

As we shall demonstrate in the numerical analysis presented in Section 3, the SUSY-QCD radiative corrections are indeed sizeable at large t_β . After summation of the t_β -enhanced terms, however, the remaining one-loop SUSY-QCD corrections are negligibly small, at the level of per mille and below.

2.3 Electroweak SM corrections and calculational details

The electroweak corrections naturally decompose into a purely photonic, QED-like part δ_{QED} and the remaining weak contributions δ_{weak} : $\delta_{\text{ew}} = \delta_{\text{QED}} + \delta_{\text{weak}}$. Each of these contributions forms a gauge-invariant subset of the $\mathcal{O}(\alpha)$ -corrected cross section. The photonic corrections due to virtual photon exchange and real photon emission can be obtained from the QCD results by appropriately adjusting colour factors and electric charges. For the QED renormalization of the bottom mass we use the on-shell scheme, because electroweak running effects beyond the one-loop level are negligible.

The divergences due to collinear photon emission from the massless b-quarks are removed by mass factorization as in QCD, i.e. by a redefinition of the bottom parton densities according to

$$f_b(x) \rightarrow f_b(x, \mu_F) + \int_x^1 \frac{dz}{z} f_b\left(\frac{x}{z}, \mu_F\right) Q_b^2 \frac{\alpha}{2\pi} \left\{ [P_{qq}(z)]_+ \left(\Delta + \ln \frac{\mu^2}{\mu_F^2} \right) - C_{qq}(z) \right\} \\ + \int_x^1 \frac{dz}{z} f_\gamma\left(\frac{x}{z}, \mu_F\right) 3 Q_b^2 \frac{\alpha}{2\pi} \left\{ P_{q\gamma}(z) \left(\Delta + \ln \frac{\mu^2}{\mu_F^2} \right) - C_{q\gamma}(z) \right\}, \quad (2.16)$$

where $\Delta = 1/\epsilon - \gamma_E + \ln(4\pi)$ is the standard divergence in $D = 4 - 2\epsilon$ dimensions, γ_E is Euler's constant, $Q_b = -1/3$ is the electric b charge, and μ_F denotes the QED factorization scale which is identified with the QCD factorization scale but is chosen independently of the scale μ introduced by dimensional regularization. The factor 3 in the second line stems from the splitting of the photon into $b\bar{b}$ -pairs of different colour. Furthermore,

$$P_{qq}(z) = \frac{1+z^2}{1-z} \quad \text{and} \quad P_{q\gamma}(z) = z^2 + (1-z)^2 \quad (2.17)$$

are the quark and photon splitting functions, respectively, and C_{qq} , $C_{q\gamma}$ the coefficient functions specifying the factorization scheme. Following standard QCD terminology one distinguishes $\overline{\text{MS}}$ and DIS schemes defined by

$$\begin{aligned}
C_{qq}^{\overline{\text{MS}}}(z) &= C_{q\gamma}^{\overline{\text{MS}}}(z) = 0, \\
C_{qq}^{\text{DIS}}(z) &= \left[P_{qq}(z) \left(\ln \frac{1-z}{z} - \frac{3}{4} \right) + \frac{9+5z}{4} \right]_+, \\
C_{q\gamma}^{\text{DIS}}(z) &= P_{q\gamma}(z) \ln \frac{1-z}{z} - 8z^2 + 8z - 1.
\end{aligned}
\tag{2.18}$$

The equivalent factorization procedure using fermion masses as regulators instead of dimensional regularization can, e.g., be found in Ref. [22]. In our numerical analysis we employ the MRST2004qed parton distribution functions [23], which include $\mathcal{O}(\alpha)$ corrections defined in the DIS factorization scheme [22]. The MRST2004qed parameterization also provides a photon density necessary to compute the hadronic cross section for the $\mathcal{O}(\alpha)$ photon-induced processes $\gamma b \rightarrow \phi^0 b$ and $\gamma \bar{b} \rightarrow \phi^0 \bar{b}$.

We have calculated the NLO QCD and QED corrections using dimensional regularization and alternatively using a mass regularization for the collinear divergences, where we employed the methods of Refs. [22, 24] for the mass regulators.

Similar to the QCD case, the QED corrections are universal for the production of SM and MSSM Higgs bosons. Their size is quite small since the potentially large correction due to collinear photon emission is absorbed into the parton distribution function $f_b(x, \mu_F)$. We shall discuss numerical results in Section 3.

Let us now turn to the remaining electroweak corrections δ_{weak} . As we shall discuss in more detail in Section 3.4, the small but finite bottom mass can induce sizeable corrections in the electroweak sector of the MSSM due to additional (t_β -enhanced) bottom Yukawa couplings in loops. Hence, while we neglect the b-mass at tree level and for the QCD and QED corrections as required by QCD factorization, we keep the finite bottom mass m_b in the calculation of the relative one-loop weak correction δ_{weak} . Thus, our result for δ_{weak} also contains kinematical m_b effects that formally lie beyond the accuracy of the 5FNS-calculation. However, these effects are small. Different choices for the numerical value of the bottom mass used within the calculation of the relative one-loop correction lead to results which formally differ by NNLO effects. Because the m_b -dependence is dominated by the strength of the Yukawa coupling, we have chosen the running bottom mass (as defined after summation of t_β -enhanced terms) as input.

Both in the SM and in the MSSM, the one-loop electroweak corrections have been calculated independently using two different approaches: In one approach, the Feynman-diagrammatic expressions for all self-energies and one-loop vertex diagrams have been generated using the program package `FeynArts` [25]. The calculations have then been performed with the help of the program package `FormCalc` [26], and the loop integrals have been evaluated numerically with `LoopTools` [26]. In a second approach, also starting from the amplitudes generated by `FeynArts`, all calculations, including the evaluation of the loop integrals, have been performed with a completely independent set of in-house routines. The two calculations are in mutual agreement. We note that the regularization of the complete electroweak MSSM corrections has been performed using both constrained differential renormalization as implemented in `FormCalc` as well as dimensional reduction. Both regularization procedures are known to be equivalent at the one-loop level [26], and the results of the two calculations are in agreement. We refrain from displaying the complete analytic results and restrict ourselves to a discussion of the renormalization conditions and the input-parameter schemes.

Using standard notation, the vertex counterterm at one-loop order is given by

$$\delta_{\text{CT}}^{\text{bb}\bar{\text{b}}\text{H}} = \delta Z_e + \frac{\delta Z_H}{2} + \frac{\delta m_b}{m_b} + \frac{\delta Z_L^{\text{b}} + \delta Z_R^{\text{b}}}{2} - \frac{\delta s_w}{s_w} - \frac{\delta M_W^2}{2M_W^2}. \quad (2.19)$$

Employing the on-shell renormalization scheme, this results in

$$\begin{aligned} \delta_{\text{CT}}^{\text{bb}\bar{\text{b}}\text{H}} = & \delta Z_e + \frac{\delta Z_H}{2} + \Sigma_S^{\text{b}}(m_b^2) - 2m_b^2 \left(\Sigma_S^{\prime\text{b}}(m_b^2) + \Sigma_V^{\prime\text{b}}(m_b^2) \right) \\ & + \frac{1}{2} \left(\frac{c_w^2 - s_w^2}{s_w^2} \frac{\Sigma_W(M_W^2)}{M_W^2} - \frac{c_w^2}{s_w^2} \frac{\Sigma_Z(M_Z^2)}{M_Z^2} \right), \end{aligned} \quad (2.20)$$

where $\Sigma_{S,V}^{\text{b}}$ denotes the scalar and vector part of the b-quark self-energy, respectively, and Σ' refers to the derivative of the self-energy with respect to the external momentum squared. The relation $s_w^2 = 1 - M_W^2/M_Z^2$ is used to determine δs_w . Here and in Section 2.4 we only consider the real part of the self-energies and follow the conventions of Ref. [27]. For compactness, the transverse parts of gauge-boson self-energies are simply written as Σ_W, Σ_Z , etc.

The different input-parameter schemes are specified by the choice of δZ_e . In the $\alpha(0)$ -scheme, using the low-energy fine-structure constant $\alpha(0)$ as input, we have [28]¹

$$\delta Z_e|_{\alpha(0)} = \frac{1}{2} \Sigma_\gamma'(0) + \frac{s_w}{c_w} \frac{\Sigma_{\gamma Z}(M_Z^2)}{M_Z^2}. \quad (2.21)$$

In the $\alpha(0)$ -scheme, δZ_e contains logarithms of the light fermion masses inducing large corrections of the form $\alpha \ln(m_f^2/\hat{s})$, which are related to the running of the electromagnetic coupling $\alpha(Q)$ from $Q = 0$ to a high energy scale. In order to correctly reproduce the non-perturbative hadronic part in this running, which enters via $\Pi_\gamma(M_Z^2) - \Pi_\gamma(0)$ with $\Pi_\gamma(k^2) = \Sigma_\gamma(k^2)/k^2$ denoting the photonic vacuum polarization, we adjust the quark masses to the asymptotic tail of $\Pi_\gamma(k^2)$. In the $\alpha(M_Z)$ -scheme, using $\alpha(M_Z)$ as defined in Ref. [29] as input, this adjustment is implicitly incorporated, and the counterterm reads

$$\delta Z_e|_{\alpha(M_Z)} = \delta Z_e|_{\alpha(0)} - \frac{1}{2} \Delta\alpha(M_Z^2), \quad (2.22)$$

where

$$\Delta\alpha(Q^2) = \Pi_\gamma^{f \neq t}(0) - \text{Re} \Pi_\gamma^{f \neq t}(Q^2), \quad (2.23)$$

and $\Pi_\gamma^{f \neq t}$ denotes the photonic vacuum polarization induced by all fermions other than the top quark. Hence, in the $\alpha(M_Z)$ -scheme, the final result does not depend on the above logarithms of the light fermion masses. In the G_μ -scheme, α is determined from the muon-decay constant G_μ according to

$$\alpha_{G_\mu} = \frac{\sqrt{2} G_\mu M_W^2 s_w^2}{\pi} = \alpha(0)(1 + \Delta r). \quad (2.24)$$

The radiative QED corrections for muon decay in the framework of the effective 4-fermion interaction are already encoded in the numerical value for G_μ . The additional corrections from a full one-loop SM calculation are taken into account through Δr [30] according to

$$\delta Z_e|_{G_\mu} = \delta Z_e|_{\alpha(0)} - \frac{1}{2} \Delta r. \quad (2.25)$$

¹We follow the convention of Haber and Kane [14] to define the covariant derivative for $\text{SU}(2)_L$, i.e. the sign in front of $\Sigma_{\gamma Z}$ in (2.21) differs from Ref. [28].

Since $\Delta\alpha(M_Z^2)$ is explicitly contained in Δr , the large fermion-mass logarithms are also absent in the G_μ -scheme. Moreover, since the lowest-order cross section is proportional to α/s_W^2 for the production of all the three Higgs bosons, in G_μ -parameterization it absorbs the large universal correction $\Delta\rho$ from the ρ -parameter, which is $\propto G_\mu m_t^2$ and represents a part of Δr . Dividing Eq. (2.24) by s_W^2 , one easily sees that α_{G_μ}/s_W^2 absorbs Δr and thus also $\Delta\rho$. We will use the G_μ -scheme unless stated otherwise. We have also performed two independent calculations for Δr in the MSSM, using either constrained differential renormalization or dimensional reduction, and find agreement with the result of Ref. [31].

In the SM, the Higgs mass can be defined by an on-shell renormalization condition. The wave-function renormalization of the Higgs-boson field is conveniently chosen in the on-shell scheme,

$$\delta Z_H = -\Sigma'_H(M_H^2), \quad (2.26)$$

where Σ_H is the Higgs-boson self-energy.

2.4 Electroweak MSSM corrections

The photonic corrections in the MSSM do not change with respect to the SM case. For the conventions and for the renormalization of the MSSM Higgs sector, which is more involved, we essentially follow Ref. [27].² In particular, a proper renormalization scheme has to be specified to determine the vertex counterterm $\delta_{CT}^{b\bar{b}H}$, cf. (2.19), including the renormalization of t_β . The wave-function renormalization for the Higgs doublet fields is usually defined by

$$H_i \rightarrow Z_{H_i}^{1/2} H_i = H_i \left(1 + \frac{1}{2} \delta Z_{H_i} \right) \quad (2.27)$$

with $i = u, d$. For the vacuum expectation values of the Higgs fields one defines

$$v_i \rightarrow Z_{H_i}^{1/2} (v_i - \delta v_i) = v_i \left(1 + \frac{1}{2} \delta Z_{H_i} - \frac{\delta v_i}{v_i} \right), \quad (2.28)$$

where the last equation is valid to one-loop order with $Z_{H_i} = 1 + \delta Z_{H_i}$. The freedom of wave-function renormalization can then be used to impose the condition

$$\frac{\delta v_u}{v_u} = \frac{\delta v_d}{v_d} \quad (2.29)$$

leading to

$$\frac{\delta t_\beta}{t_\beta} = \frac{1}{2} (\delta Z_{H_u} - \delta Z_{H_d}). \quad (2.30)$$

Hence, for the MSSM Higgs sector the counterterm δZ_H in (2.19) reads

$$\delta Z_H = \frac{1}{2} \delta Z_{H_d} + s_\beta^2 \frac{\delta t_\beta}{t_\beta} = \frac{1}{2} (c_\beta^2 \delta Z_{H_d} + s_\beta^2 \delta Z_{H_u}). \quad (2.31)$$

Note, that δZ_H includes all parts of the vertex counterterm that are related to the Higgs sector, i.e. δt_β as well as the wave-function renormalization counterterm δZ_{H_d} . The quantity δZ_H should

²For clarity, we specify our conventions for some field-theoretic quantities where the conventions of Ref. [27] might be unclear. Explicit tadpole vertex functions for Higgs fields are denoted as $\Gamma^{\phi^0} = iT^{\phi^0}$, i.e. T^{ϕ^0} differs from Ref. [27] by a global sign. The $A^0 Z$ mixing self-energy is derived from the vertex function $\Gamma_\mu^{A^0 Z}(k, -k) = k_\mu \Sigma_{A^0 Z}(k^2)$, where k is the incoming A^0 momentum.

not be confused with the wave-function renormalization constants for the physical Higgs fields. Since the counterterm δZ_H is universal for the production of h^0 , H^0 , and A^0 via down-type quarks, the whole vertex counterterm $\delta_{\text{CT}}^{\text{b}\bar{\text{b}}\text{H}}$ (2.19) is also universal.

We consider two renormalization schemes for t_β :

- i) Following Dabelstein [27] and Chankowski et al. [32], a vanishing on-shell $A^0 Z$ -mixing can be used as a renormalization condition, i.e.

$$\hat{\Sigma}_{A^0 Z}(M_{A^0}^2) = 0, \quad (2.32)$$

where

$$\hat{\Sigma}_{A^0 Z}(k^2) = \Sigma_{A^0 Z}(k^2) - M_Z s_{2\beta} \frac{\delta t_\beta}{t_\beta} \quad (2.33)$$

denotes the real part of a renormalized self-energy defined according to the conventions in Ref. [27]. To fix the second wave-function renormalization constant, one demands the on-shell condition

$$\hat{\Sigma}'_{A^0}(M_{A^0}^2) = 0 \quad (2.34)$$

for the residue of the A^0 -boson propagator. From the last two equations, one finds

$$\begin{aligned} \delta Z_{H_u} &= -\Sigma'_{A^0}(M_{A^0}^2) + \frac{t_\beta}{M_Z} \Sigma_{A^0 Z}(M_{A^0}^2), \\ \delta Z_{H_d} &= -\Sigma'_{A^0}(M_{A^0}^2) - \frac{1}{t_\beta M_Z} \Sigma_{A^0 Z}(M_{A^0}^2), \end{aligned} \quad (2.35)$$

which defines the DCPR scheme [27, 32] for the t_β renormalization [see (2.30)].

- ii) Alternatively, in the $\overline{\text{DR}}$ scheme, the counterterm for t_β is proportional to $\Delta = 1/\epsilon - \gamma_E + \ln(4\pi)$. Hence, one can convert (2.35) to the $\overline{\text{DR}}$ scheme by setting the remaining finite pieces of $\Sigma_{A^0 Z}$ to zero. Accordingly, $t_\beta^{\overline{\text{DR}}}$ is a renormalization-scale-dependent quantity, i.e. the input for a given model has to be fixed at a given scale μ_R . To one-loop order, the conversion of the t_β input parameters from the $\overline{\text{DR}}$ scheme to t_β^{DCPR} in the DCPR scheme is given by

$$\left[t_\beta + \frac{1}{2M_Z c_\beta^2} \Sigma_{A^0 Z}^{\text{fin}}(M_{A^0}^2) \right]^{\text{DCPR}} = t_\beta^{\overline{\text{DR}}}, \quad (2.36)$$

where Σ^{fin} denotes the finite pieces of the self-energy in the $\overline{\text{DR}}$ scheme. In this work, we always use the renormalization condition (2.34), also if we use $\overline{\text{DR}}$ to renormalize t_β .

In analogy, there are the DCPR and the $\overline{\text{DR}}$ schemes for the renormalization of the mass M_{A^0} of the pseudoscalar Higgs boson. The DCPR scheme uses the on-shell renormalization condition

$$\hat{\Sigma}_{A^0}(M_{A^0}^2) = 0, \quad (2.37)$$

while the $\overline{\text{DR}}$ scheme is again defined by setting $\Sigma_{A^0}^{\text{fin}}(M_{A^0}^2)$ to zero in the mass counterterm for the pseudoscalar Higgs boson. In this work, we use the on-shell scheme for the renormalization of A^0 . Supersymmetric models are usually defined in terms of $\overline{\text{DR}}$ parameters [33]. Hence, we have to calculate the on-shell A^0 mass from the corresponding scale-dependent $\overline{\text{DR}}$ parameter. For a given parameter set, we determine $M_{A^0}^{\text{os}}$ from the zero of the inverse A^0 propagator³

$$(M_{A^0}^{\text{os}})^2 - (M_{A^0}^{\overline{\text{DR}}})^2 + \Sigma_{A^0}^{\text{fin}}((M_{A^0}^{\text{os}})^2) = 0 \quad (2.38)$$

³In contrast to Ref. [19], but in line with Ref. [33], we assume that all tadpole contributions to the mass of A^0 are absorbed in the definition of the $\overline{\text{DR}}$ mass $M_{A^0}^{\overline{\text{DR}}}$.

which corresponds to a given $\overline{\text{DR}}$ mass for A^0 . Here, $\Sigma_{A^0}^{\text{fin}}(k^2)$ is calculated from an MSSM parameter set using $M_{A^0}^{\text{os}}$ as input. We start with $M_{A^0}^{\text{os}} = M_{A^0}^{\text{DR}}$ for the self-energy calculation and iterate until self-consistency is reached. If t_β is renormalized in the DCPR scheme, (2.36) is used to also find t_β^{DCPR} self-consistently along with $M_{A^0}^{\text{os}}$. The one-loop shift of the numerical value of M_{A^0} is particularly important because it enters already at tree level through the determination of the mixing angle [see (2.6)].

For completeness, we also state the remaining renormalization conditions for the tadpoles,

$$T_{h^0} + \delta t_{h^0} = 0 \quad \text{and} \quad T_{H^0} + \delta t_{H^0} = 0, \quad (2.39)$$

which ensure that v_u and v_d correctly minimize the one-loop potential. As in the SM, the masses for the W and Z boson are renormalized by on-shell conditions.

Including the corrections to the Higgs external legs, the partonic cross section to one-loop order is given by

$$\begin{aligned} \sigma_{h^0}^{(1)} &= \sigma_{h^0}^{\text{tree}} \cdot Z_{h^0} \left[\left(1 - Z_{h^0 H^0} \frac{c_\alpha}{s_\alpha} \right)^2 + 2 \operatorname{Re} \left(1 - Z_{h^0 H^0} \frac{c_\alpha}{s_\alpha} \right) \Delta_{h^0} \right], \\ \sigma_{H^0}^{(1)} &= \sigma_{H^0}^{\text{tree}} \cdot Z_{H^0} \left[\left(1 - Z_{H^0 h^0} \frac{s_\alpha}{c_\alpha} \right)^2 + 2 \operatorname{Re} \left(1 - Z_{H^0 h^0} \frac{s_\alpha}{c_\alpha} \right) \Delta_{H^0} \right], \\ \sigma_{A^0}^{(1)} &= \sigma_{A^0}^{\text{tree}} \cdot Z_{A^0} (1 + 2 \operatorname{Re} \Delta_{A^0}), \end{aligned} \quad (2.40)$$

where Δ_{ϕ^0} denotes the relative one-loop vertex corrections including the corresponding counterterms. Depending on the renormalization scheme, Δ_{A^0} also includes the contributions from ZA^0 -mixing and G^0A^0 -mixing. The Z factors are given by [12]

$$\begin{aligned} Z_{h^0} &= \frac{1}{1 + \hat{\Sigma}'_{h^0}(k^2) - \left(\frac{\hat{\Sigma}_{H^0 h^0}^2(k^2)}{k^2 - m_{H^0}^2 + \hat{\Sigma}_{H^0}(k^2)} \right)'} \Bigg|_{k^2=M_{h^0}^2}, \\ Z_{H^0} &= \frac{1}{1 + \hat{\Sigma}'_{H^0}(k^2) - \left(\frac{\hat{\Sigma}_{H^0 h^0}^2(k^2)}{k^2 - m_{h^0}^2 + \hat{\Sigma}_{h^0}(k^2)} \right)'} \Bigg|_{k^2=M_{H^0}^2}, \\ Z_{A^0} &= \frac{1}{1 + \hat{\Sigma}'_{A^0}(k^2)} \Bigg|_{k^2=M_{A^0}^2} = 1. \end{aligned} \quad (2.41)$$

The mixing of the CP-even Higgs bosons is determined by

$$\begin{aligned} Z_{h^0 H^0} &= - \frac{\hat{\Sigma}_{H^0 h^0}(M_{h^0}^2)}{M_{h^0}^2 - m_{H^0}^2 + \hat{\Sigma}_{H^0}(M_{h^0}^2)}, \\ Z_{H^0 h^0} &= - \frac{\hat{\Sigma}_{H^0 h^0}(M_{H^0}^2)}{M_{H^0}^2 - m_{h^0}^2 + \hat{\Sigma}_{h^0}(M_{H^0}^2)}, \end{aligned} \quad (2.42)$$

where m_{ϕ^0} denotes the tree-level masses and M_{ϕ^0} the one-loop masses ($\phi^0 = h^0, H^0$), i.e. the zeros of the inverse one-loop propagator matrix determinant

$$\left(k^2 - m_{h^0}^2 + \hat{\Sigma}_{h^0}(k^2) \right) \left(k^2 - m_{H^0}^2 + \hat{\Sigma}_{H^0}(k^2) \right) - \hat{\Sigma}_{H^0 h^0}^2(k^2) = 0. \quad (2.43)$$

The renormalized Higgs self-energies in turn are given by

$$\begin{aligned}
\hat{\Sigma}_{h^0}(k^2) &= \Sigma_{h^0}(k^2) + k^2 (\delta Z_{H_u} c_\alpha^2 + \delta Z_{H_d} s_\alpha^2) - \delta m_{h^0}^2, \\
\hat{\Sigma}_{H^0}(k^2) &= \Sigma_{H^0}(k^2) + k^2 (\delta Z_{H_u} s_\alpha^2 + \delta Z_{H_d} c_\alpha^2) - \delta m_{H^0}^2, \\
\hat{\Sigma}_{H^0 h^0}(k^2) &= \Sigma_{H^0 h^0}(k^2) + k^2 s_\alpha c_\alpha (\delta Z_{H_u} - \delta Z_{H_d}) - \delta m_{H^0 h^0}^2,
\end{aligned} \tag{2.44}$$

where the Higgs mass counterterms read⁴

$$\begin{aligned}
\delta m_{h^0}^2 &= c_{\beta-\alpha}^2 \Sigma_{A^0}(M_{A^0}^2) + s_{\beta+\alpha}^2 \Sigma_Z(M_Z^2) - \frac{e s_{\beta-\alpha}^2 c_{\beta-\alpha}}{2M_Z s_W c_W} T_{H^0} + \frac{e s_{\beta-\alpha} (1 + c_{\beta-\alpha}^2)}{2M_Z s_W c_W} T_{h^0} \\
&\quad - (M_{A^0}^2 c_{\beta-\alpha}^2 + M_Z^2 s_{\beta+\alpha}^2) \Sigma'_{A^0}(M_{A^0}^2) + M_Z \frac{c_{2\alpha} - c_{2\beta}}{s_{2\beta}} \Sigma_{A^0 Z}(M_{A^0}^2),
\end{aligned} \tag{2.45}$$

$$\begin{aligned}
\delta m_{H^0}^2 &= s_{\beta-\alpha}^2 \Sigma_{A^0}(M_{A^0}^2) + c_{\beta+\alpha}^2 \Sigma_Z(M_Z^2) + \frac{e c_{\beta-\alpha} (1 + s_{\beta-\alpha}^2)}{2M_Z s_W c_W} T_{H^0} - \frac{e c_{\beta-\alpha}^2 s_{\beta-\alpha}}{2M_Z s_W c_W} T_{h^0} \\
&\quad - (M_{A^0}^2 s_{\beta-\alpha}^2 + M_Z^2 c_{\beta+\alpha}^2) \Sigma'_{A^0}(M_{A^0}^2) - M_Z \frac{c_{2\alpha} + c_{2\beta}}{s_{2\beta}} \Sigma_{A^0 Z}(M_{A^0}^2),
\end{aligned} \tag{2.46}$$

$$\begin{aligned}
\delta m_{H^0 h^0}^2 &= -\frac{s_{2(\beta-\alpha)}}{2} \Sigma_{A^0}(M_{A^0}^2) - \frac{s_{2(\beta+\alpha)}}{2} \Sigma_Z(M_Z^2) + \frac{e s_{\beta-\alpha}^3}{2M_Z s_W c_W} T_{H^0} + \frac{e c_{\beta-\alpha}^3}{2M_Z s_W c_W} T_{h^0} \\
&\quad + \frac{1}{2} (M_{A^0}^2 s_{2(\beta-\alpha)} + M_Z^2 s_{2(\beta+\alpha)}) \Sigma'_{A^0}(M_{A^0}^2) + M_Z \frac{s_{2\alpha}}{s_{2\beta}} \Sigma_{A^0 Z}(M_{A^0}^2).
\end{aligned} \tag{2.47}$$

If t_β is renormalized in the $\overline{\text{DR}}$ scheme the finite parts of $\Sigma_{A^0 Z}$ have to be set to zero in the above formulas. Note also that M_{A^0} is the on-shell A^0 -mass in these formulas, because we translate the M_{A^0} input always to the on-shell scheme before the actual loop calculation. As mentioned before, in all the above equations we only consider the real parts of the self-energies. Neglecting the imaginary part does not spoil the one-loop accuracy of our calculation, since the imaginary parts formally only enter at higher orders.⁵

In complete analogy to SUSY-QCD in Section 2.2, there are t_β -enhanced corrections in the electroweak sector which can be numerically sizeable and which should be summed [20] to all orders. Higgsino–stop loops lead to a contribution to Δ_b of the form

$$\Delta_b^{\tilde{H}\tilde{t}} = \frac{\alpha m_t^2}{8\pi s_W^2 s_\beta^2 M_W^2} A_t \mu t_\beta I(m_{\tilde{t}_1}, m_{\tilde{t}_2}, \mu), \tag{2.48}$$

where $m_{\tilde{t}_i}^2$ denote the masses of the stop mass eigenstates, and A_t is the usual trilinear soft breaking parameter. From wino–higgsino–stop and wino–higgsino–sbottom loops we find

$$\begin{aligned}
\Delta_b^{\tilde{W}} &= -\frac{\alpha}{8\pi s_W^2} M_2 \mu t_\beta \left[2 \cos^2 \Theta_{\tilde{t}} I(m_{\tilde{t}_1}, \mu, M_2) + 2 \sin^2 \Theta_{\tilde{t}} I(m_{\tilde{t}_2}, \mu, M_2) \right. \\
&\quad \left. + \cos^2 \Theta_{\tilde{b}_1} I(m_{\tilde{b}_1}, \mu, M_2) + \sin^2 \Theta_{\tilde{b}_2} I(m_{\tilde{b}_2}, \mu, M_2) \right],
\end{aligned} \tag{2.49}$$

⁴Up to some (known) sign errors in $\delta m_{H^0 h^0}^2$, the Higgs mass counterterms can be also found in Ref. [27].

⁵While an inclusion of such imaginary parts in mass determinations of unstable particles is straightforward, a consistent inclusion of such width effects in the description of particle reactions requires an inspection of full resonance processes including production and decay of the unstable particles. This is beyond the aimed level of precision of this work.

where M_2 is the soft SUSY-breaking mass parameter for the wino, $\Theta_{\tilde{t}}$ denotes the stop mixing angle, and the auxiliary function $I(a, b, c)$ is given in (2.12). Finally, bino loops contribute

$$\Delta_{\tilde{b}}^{\tilde{B}} = -\frac{\alpha}{72\pi c_W^2} M_1 \mu t_\beta \left[3(1 + \sin^2 \Theta_{\tilde{b}}) I(m_{\tilde{b}_1}, \mu, M_1) + 3(1 + \cos^2 \Theta_{\tilde{b}}) I(m_{\tilde{b}_2}, \mu, M_1) + 2I(m_{\tilde{b}_1}, m_{\tilde{b}_2}, M_1) \right], \quad (2.50)$$

where M_1 is the soft SUSY-breaking mass parameter for the bino. The full result for $\Delta_{\tilde{b}}$ is then given by

$$\Delta_{\tilde{b}} = \Delta_{\tilde{b}}^{\tilde{g}} + \Delta_{\tilde{b}}^{\text{weak}} = \Delta_{\tilde{b}}^{\tilde{g}} + \Delta_{\tilde{b}}^{\tilde{H}\tilde{t}} + \Delta_{\tilde{b}}^{\tilde{W}} + \Delta_{\tilde{b}}^{\tilde{B}}, \quad (2.51)$$

where $\Delta_{\tilde{b}}^{\tilde{g}}$ denotes the gluino contribution of (2.11). We have recalculated these results and find agreement with Ref. [20]. In contrast to Ref. [20] we also include the bino terms in the summation. However, they are indeed numerically small.

To further improve the accuracy of the calculation, we also include two-loop contributions to the self-energies as provided by the program package `FeynHiggs` [35] (version 2.3.2). As for the one-loop part of the self-energies we find perfect agreement between our calculation and the results obtained with `FeynHiggs`.⁶

In addition to using a properly defined b-mass, one often absorbs parts of the radiative correction related to the Higgs external leg using an effective mixing angle $\alpha_{\text{eff}} = \alpha + \delta\alpha$ at tree level. Here, we follow `FeynHiggs` and define $\delta\alpha$ to be the angle which diagonalizes the loop-corrected Higgs mass matrix, i.e.

$$\begin{pmatrix} m_{h^0}^2 - \hat{\Sigma}_{h^0}(m_{h^0}^2) & -\hat{\Sigma}_{h^0 H^0}((m_{h^0}^2 + m_{H^0}^2)/2) \\ -\hat{\Sigma}_{h^0 H^0}((m_{h^0}^2 + m_{H^0}^2)/2) & m_{H^0}^2 - \hat{\Sigma}_{H^0}(m_{H^0}^2) \end{pmatrix} \xrightarrow{\delta\alpha} \begin{pmatrix} M_{h^0}^2 & 0 \\ 0 & M_{H^0}^2 \end{pmatrix}, \quad (2.52)$$

where the renormalized Higgs self-energies are evaluated at the given momenta. We define an improved Born approximation σ_{IBA} which includes the leading higher-order corrections through the running b-mass, the summation of t_β -enhanced terms and the effective mixing angle,

$$\hat{\sigma}_{\text{IBA}} = \frac{\sqrt{2}\pi G_\mu \overline{m}_b(\mu_R)^2}{6M_{\phi^0}^2} \delta(1 - \tau) \begin{cases} \frac{s_{\alpha_{\text{eff}}}^2}{c_\beta^2} \left(\frac{1 - \Delta_{\tilde{b}}/(t_\beta t_{\alpha_{\text{eff}}})}{1 + \Delta_{\tilde{b}}} \right)^2, & h^0 \\ \frac{c_{\alpha_{\text{eff}}}^2}{c_\beta^2} \left(\frac{1 + \Delta_{\tilde{b}} t_{\alpha_{\text{eff}}}/t_\beta}{1 + \Delta_{\tilde{b}}} \right)^2, & \text{for } H^0 \text{ production,} \\ t_\beta^2 \left(\frac{1 - \Delta_{\tilde{b}}/t_\beta^2}{1 + \Delta_{\tilde{b}}} \right)^2 & A^0 \end{cases} \quad (2.53)$$

where $\hat{\sigma}_{\text{IBA}}$ denotes the partonic cross section, $\phi^0 = (h^0, H^0, A^0)$, $\tau = M_{\phi^0}^2/\hat{s}$, and $\sqrt{\hat{s}}$ is the partonic CMS energy. Here $\overline{m}_b(\mu_R)$ is the running $\overline{\text{MS}}$ bottom mass in QCD, $\Delta_{\tilde{b}}$ comprises the t_β -enhanced terms of the supersymmetric QCD and weak corrections as specified in (2.51), and α_{eff} is the effective mixing angle defined in (2.52). We will compare our full result to this approximation in Section 3.

⁶Since `FeynHiggs` does not directly support our renormalization scheme ii) (the Higgs field renormalization is different), we had to implement this scheme in `FeynHiggs` ourselves. For the leading two-loop corrections included in `FeynHiggs`, neither $\tan\beta$ nor the Higgs fields are renormalized at the two-loop level. Thus, it is consistent to add the `FeynHiggs` two-loop correction to the one-loop result in our renormalization schemes.

3 Phenomenological analysis

3.1 SM input parameters

For our numerical predictions, we essentially use the SM input parameters [36]

$$\begin{aligned}
 \alpha &= 1/137.03599911, & \alpha(M_Z) &= 1/128.952, & G_\mu &= 1.16637 \times 10^{-5} \text{ GeV}^{-2}, \\
 M_W &= 80.403 \text{ GeV}, & M_Z &= 91.1876 \text{ GeV}, \\
 m_e &= 0.51099892 \text{ MeV}, & m_\mu &= 105.658369 \text{ MeV}, & m_\tau &= 1.77699 \text{ GeV}, \\
 m_u &= 66 \text{ MeV}, & m_c &= 1.2 \text{ GeV}, & m_t &= 174.2 \text{ GeV}, \\
 m_d &= 66 \text{ MeV}, & m_s &= 0.15 \text{ GeV}, & \overline{m}_b(\overline{m}_b) &= 4.2 \text{ GeV}.
 \end{aligned}
 \tag{3.1}$$

Here, $\overline{m}_b(\overline{m}_b)$ is the QCD- $\overline{\text{MS}}$ mass for the bottom quark while the top mass m_t is understood as an on-shell mass. For the QED renormalization of the bottom mass we use the on-shell scheme, as mentioned above, with an on-shell mass $m_b = 4.53 \text{ GeV}$ calculated from $\overline{m}_b(\overline{m}_b)$ to one-loop order in QCD. The masses of the light quarks are adjusted such as to reproduce the hadronic contribution to the photonic vacuum polarization leading to $\alpha(M_Z)$ of Ref. [37]. They are relevant only for the evaluation of the charge renormalization constant δZ_e in the $\alpha(0)$ -scheme. The CKM matrix has been set to the unit matrix. For the calculation of the hadronic cross sections we have adopted the MRST2004qed parton distribution functions [23] at NLO QCD and NLO QED, with the corresponding $\alpha_s(M_Z) = 0.11899$. The top quark, squarks, and gluinos are decoupled from the running of the strong coupling $\alpha_s(\mu_R)$. We choose the renormalization and factorization scales as $\mu_R = M_H$ and $\mu_F = M_H/4$, respectively. As mentioned above, with this specific choice the QCD NNLO radiative corrections are at the percent level [11].

3.2 The SM cross section

The NLO cross section predictions for associated $b\bar{b}H$ production at the LHC, including QCD, QED and weak corrections, are shown in Table 1 for the three different input-parameter schemes introduced in Section 2.3. The QED corrections are very small after potentially large contributions from collinear photon emission have been removed by mass factorization as described in Section 2.3. As expected, the inclusion of the electroweak corrections reduces the scheme dependence. In the following we will adopt the G_μ -scheme, where the value of the electromagnetic coupling is derived from muon decay according to α_{G_μ} and where the influence of the light-quark masses is negligible. Note that the relative $\mathcal{O}(\alpha)$ QED corrections are evaluated with $\alpha(0)$, irrespective of the chosen input-parameter scheme, because the relevant scale for the bremsstrahlung process is set by the vanishing virtuality of the emitted real photon.

3.3 MSSM input

For our numerical analysis, we will focus on the benchmark scenario SPS 4 [38] which is characterized by a large value of $t_\beta = 50$ and a correspondingly large associated production cross section $b\bar{b} \rightarrow H^0, A^0$ at the LHC. Results for the alternative benchmark scenario SPS 1b with $t_\beta = 30$ will be presented in Appendix B. Both the SPS 4 and SPS 1b input parameters are specified in Appendix A. Note that searches at the Fermilab Tevatron are not sensitive to scenarios with H^0, A^0 -masses as large as the masses in SPS 4 or SPS 1b.

From the SPS $\overline{\text{DR}}$ input parameters we calculate $M_{A^0}^{\text{os}}$ and, if we work in the DCPR scheme, also t_β^{DCPR} , as specified in Section 2.4. The corresponding renormalization scale $\mu_R(\overline{\text{DR}})$ used

σ [pb]	LO	QCD	QCD+QED	full SM
$\alpha(0)$ -scheme	0.02309	0.02868	0.02863	0.02901 (25.6%)
G_μ -scheme	0.02390	0.02968	0.02963	0.02924 (22.3%)
$\alpha(M_Z)$ -scheme	0.02453	0.03047	0.03042	0.02932 (19.5%)

Table 1: The LO and NLO SM cross section $pp \rightarrow (b\bar{b})H + X$ for a Higgs boson with $M_H = 300$ GeV at the LHC ($\sqrt{s} = 14$ TeV). Results are presented for the three different input-parameter schemes defined in Section 2.3. The MRST2004qed parton distribution function and NNLO-QCD running for the b-mass have been adopted for the NLO as well as the LO cross sections, and the renormalization and factorization scales have been set to $\mu_R = M_H$ and $\mu_F = M_H/4$, respectively. “QCD” denotes the NLO QCD corrections only, “QCD+QED” also includes photon exchange and emission as well as the initial state containing a photon. The “full SM” prediction includes all $\mathcal{O}(\alpha_s)$ and $\mathcal{O}(\alpha)$ corrections; the corresponding relative correction is indicated in parentheses.

in the electroweak part of the calculation is specified by the SPS scenario (see Appendix A). Note, that it differs in general from the renormalization scale in the QCD part of the calculation which is set to the mass of the produced Higgs boson. The MSSM tree-level relations are used to determine the sfermion and gaugino masses and mixing angles that enter the one-loop corrections. The Higgs masses and the Higgs sector mixing angle α [see (2.6)] which enter the calculation of the loop diagrams are also obtained according to the tree-level relations.

While the bottom mass that enters the Yukawa coupling at LO is fixed by the requirement to account for dominant NLO corrections, different definitions for the bottom mass in the relative NLO correction change the result only beyond NLO. As argued in Section 2.3, we shall use the running bottom mass as defined after summation of t_β -enhanced terms as input⁷. The running mass is needed as an input for the determination of the MSSM parameters, but it also depends on these parameters through the QCD renormalization scale $\mu_R = M_{\phi^0}$ and through the t_β -enhanced corrections. The b-mass is thus calculated using an iterative procedure, starting from some initial guess for its value, and using the resulting b-mass as input for a refined determination of the MSSM parameters, until self-consistency is reached. Note, however, that this running mass depends on the process under consideration through the choice of scale and through the t_β -enhanced corrections. In order to avoid the proliferation of input masses, we adopt the running b-mass associated with H^0 production in the relative corrections to all processes, e.g. $m_b = 2.24$ GeV for SPS 4 in the $\overline{\text{DR}}$ scheme.

We use the two-loop-improved Higgs masses for the kinematics, e.g. in the tree-level cross section or when they appear as external momenta in the on-shell vertex-correction. Using the two-loop self-energies from `FeynHiggs` [35], these two-loop improved on-shell Higgs-boson masses in the SPS 4 scenario are given by $M_{h^0} = 115.66$ GeV, $M_{H^0} = 397.72$ GeV, and $M_{A^0} = 397.67$ GeV for the renormalization scheme ii) introduced in Section 2.4, i.e. what we call $\overline{\text{DR}}$ scheme. (As described in Section 2.3 we only consider the real part of the self-energies when we determine

⁷While the electroweak corrections are calculated using dimensional reduction, we do not convert the running MS bottom mass to the corresponding $\overline{\text{DR}}$ mass to define the input value for the relative one-loop correction. The difference is of higher order.

	h^0	H^0	A^0
$\sigma_{\text{IBA}} [\text{pb}]$	0.65	15.39	15.40
$\delta_{\text{QCD}} [\%]$	36.25	21.48	21.48
$\delta_{\text{QED}} [\%]$	-0.13	-0.23	-0.23
$\delta_{\text{MSSM-QCD}} [\%]$	-0.03	0.08	0.07
$\delta_{\text{MSSM-weak}} [\%]$	-1.22	-1.57	-1.60

Table 2: LO cross section in the improved Born approximation σ_{IBA} as defined in (2.53), as well as corrections δ relative to σ_{IBA} , for $pp \rightarrow (b\bar{b}) h^0/H^0/A^0 + X$ at the LHC ($\sqrt{s} = 14$ TeV) in the SPS 4 scenario. The MRST2004qed PDFs and NNLO-QCD running for m_b have been adopted, the renormalization and factorization scales have been set to $\mu_R = M_{\phi^0}$ and $\mu_F = M_{\phi^0}/4$, respectively, and t_β has been renormalized in the $\overline{\text{DR}}$ scheme. “QCD” denotes the NLO QCD corrections only, “QED” denotes all photonic corrections only, and “MSSM-QCD” and “MSSM-weak” comprise only the QCD and weak effects in the MSSM, respectively, that remain after absorbing the large- t_β effects in the LO cross section.

the Higgs masses, in contrast to the default setting in `FeynHiggs`. Including the imaginary parts has no visible effect on M_{h^0} and shifts M_{H^0} by only approximately 200 MeV.)

3.4 The MSSM cross sections

Within the MSSM, let us first focus on the radiative corrections and total cross sections in the SPS 4 benchmark scenario using the $\overline{\text{DR}}$ scheme for the renormalization of t_β .

In Table 2 we present the relative radiative corrections δ defined with respect to the improved Born approximation σ_{IBA} defined in Eq. (2.53). The full cross-section prediction including summations and the remaining non-universal $\mathcal{O}(\alpha_s)$ and $\mathcal{O}(\alpha)$ corrections is thus given by $\sigma = \sigma_{\text{IBA}} \times (1 + \delta_{\text{QCD}} + \delta_{\text{QED}} + \delta_{\text{MSSM-QCD}} + \delta_{\text{MSSM-weak}})$. Note that we have removed corrections from our full calculation that are taken into account through the use of α_{eff} in σ_{IBA} to avoid double counting. As can be seen from Table 2, the bulk of the MSSM-QCD and -weak corrections can indeed be absorbed into the above definition of σ_{IBA} . The remaining non-universal corrections $\delta_{\text{MSSM}} = \delta_{\text{MSSM-QCD}} + \delta_{\text{MSSM-weak}}$ in the complete MSSM calculation turn out to be quite small, below approximately 2%. We note, however, that the size of the corrections δ_{MSSM} depends quite sensitively on the numerical value of the input b-mass. We shall discuss this point in more detail below.

In Table 3, we show the cumulating effect of the various higher-order corrections on the effective b-mass (as defined after summation of t_β -enhanced terms, $m_b \rightarrow m_b(1 - \Delta_b/(t_\beta t_\alpha))/(1 + \Delta_b)$ for h^0 production, etc.) and the resulting cross sections. As already observed within the SM, the QED corrections are generally very small after mass factorization. The summation of the t_β -enhanced MSSM-QCD and MSSM-weak corrections, encoded in $\Delta_b^{\hat{g}}$ and Δ_b^{weak} , respectively, has a significant effect on the cross sections for H^0 and A^0 production. The light Higgs boson h^0 , on the other hand, is SM-like in the SPS 4 scenario and the summation of terms $\propto t_\beta$ has thus no sizeable impact on the cross section. Employing a loop-improved effective mixing angle α_{eff} is numerically relevant only for h^0 production because $s_\alpha \sim -1/t_\beta$ is small and even a small shift

	h^0		H^0		A^0	
	$m_b[\text{GeV}]$	$\sigma[\text{pb}]$	$m_b[\text{GeV}]$	$\sigma[\text{pb}]$	$m_b[\text{GeV}]$	$\sigma[\text{pb}]$
QCD	2.80	0.97	2.55	24.12	2.55	24.13
+QED	2.80	0.97	2.55	24.07	2.55	24.09
$+\Delta_b^{\tilde{g}}$	2.72	0.92	1.95	14.14	1.95	14.15
$+\Delta_b^{\text{weak}}$	2.75	0.94	2.24	18.66	2.24	18.67
$+\sin(\alpha_{eff})$	2.75	0.88	2.24	18.66	2.24	18.67
full calculation	2.75	0.87	2.24	18.43	2.24	18.44

Table 3: The NLO MSSM cross section $pp \rightarrow (b\bar{b})h^0/H^0/A^0 + X$ at the LHC ($\sqrt{s} = 14$ TeV) in the SPS 4 scenario including the cumulative corrections due to the different classes of corrections (PDFs, scale setting, and t_β renormalization as in Table 2). We also quote the effective bottom mass entering the respective effective Yukawa coupling, to quantify the impact of the summation. “QCD” denotes the NLO QCD corrections only, “QED” denotes the addition of all photonic corrections, $\Delta_b^{\tilde{g}}$ and Δ_b^{weak} refer to the effect of summing t_β enhanced terms in SUSY-QCD and the weak MSSM, respectively, $\sin(\alpha_{eff})$ denotes the additional improvement of the Born cross section by using the effective mixing angle α_{eff} . Finally, we give the result for the full calculation in the MSSM where all $\mathcal{O}(\alpha_s)$ and $\mathcal{O}(\alpha)$ corrections are included.

$\alpha \rightarrow \alpha_{eff}$ has a sizeable effect on s_α . The cross sections in the last-but-one row of Table 3 correspond to the improved Born approximation dressed with QCD and QED corrections. The full MSSM cross section including all summations and the remaining non-universal $\mathcal{O}(\alpha_s)$ and $\mathcal{O}(\alpha)$ corrections is displayed in the last row of the table. As discussed previously, the non-universal supersymmetric corrections turn out to be small at a level of a few percent. Note that the b-mass values in the last row of Table 3 have been used to calculate the cross sections tabulated in Table 2. (While $m_b = 2.75$ GeV and $m_b = 2.24$ GeV have been used to calculate σ_{IBA} for h^0 and H^0/A^0 production, respectively, $m_b = 2.24$ GeV has been used as input for all relative corrections, as discussed before.)

In Fig. 2 we show the impact of the complete supersymmetric $\mathcal{O}(\alpha_s)$ and $\mathcal{O}(\alpha)$ corrections, $\delta_{\text{MSSM}} = \delta_{\text{MSSM-QCD}} + \delta_{\text{MSSM-weak}}$, defined relative to the improved Born approximation σ_{IBA} (2.53), for different values of the on-shell mass M_{A^0} . All other MSSM parameters are kept fixed to the SPS 4 values. The size of the non-universal corrections does not exceed 3% for H^0/A^0 production except for special model parameters, where the Higgs masses are close to the production threshold for pairs of sparticles. The peaks in the corrections correspond to neutralino, chargino, or sfermion thresholds. Thresholds which are too narrow, however, are not displayed in Fig. 2. These unphysical singularities can be removed by taking into account the finite widths of the unstable sparticles (see e.g. Ref. [39]). Note that the peaks for h^0 production are induced by the finite parts of the counterterms in (2.34). This proliferation of unphysical singularities can be avoided by choosing the $\overline{\text{DR}}$ scheme for the A^0 wave function renormalization, as is default in **FeynHiggs**.

For small M_{A^0} when the masses of the neutral Higgs bosons are almost degenerate, the effects from the loop-induced Higgs mixing become extremely large. To go beyond the effective

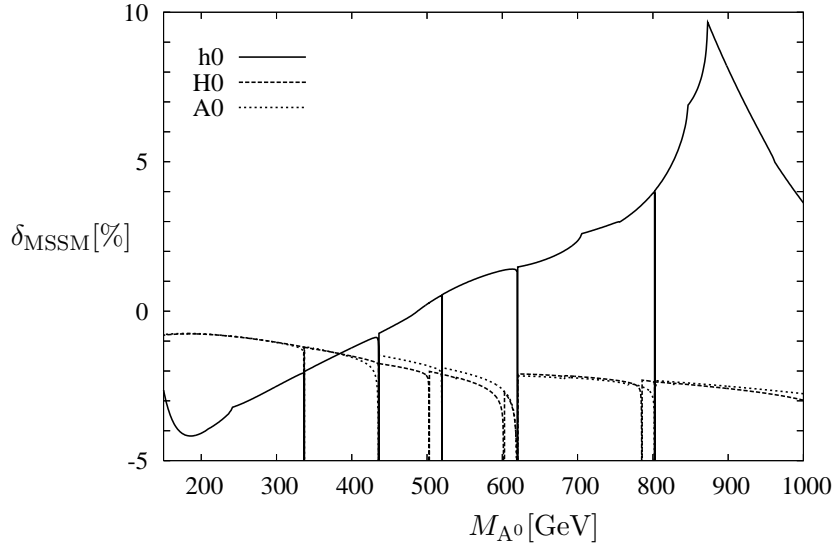


Figure 2: Full MSSM corrections $\delta_{\text{MSSM}} = \delta_{\text{MSSM-QCD}} + \delta_{\text{MSSM-weak}}$ defined relative to σ_{IBA} as a function of the M_{A^0} pole mass in the $\overline{\text{DR}}$ scheme for t_β . All other MSSM parameters are fixed to their SPS 4 values.

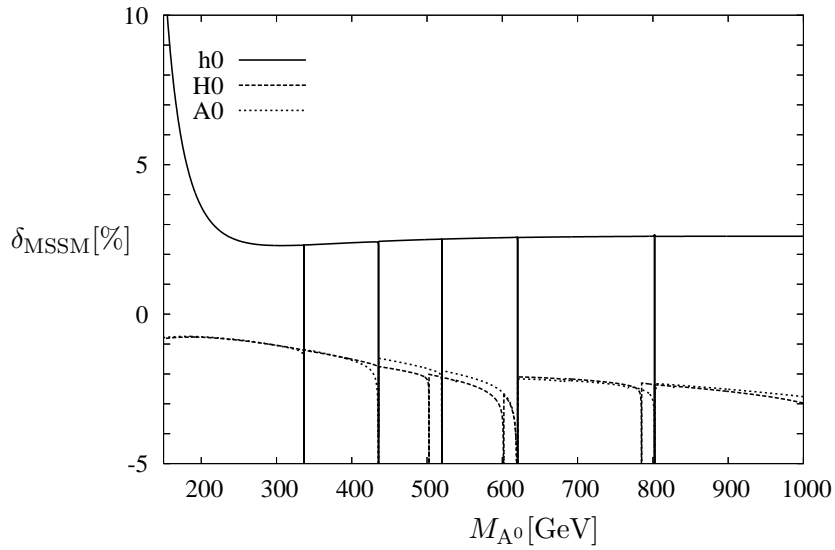


Figure 3: Full MSSM corrections $\delta_{\text{MSSM}} = \delta_{\text{MSSM-QCD}} + \delta_{\text{MSSM-weak}}$ as in Fig. 2. However, here α_{eff} (2.52) in σ_{IBA} is calculated from self-energies at $p^2 = 0$.

mixing angle approximation in this region, one would have to include corrections to the off-shell $b\bar{b}h^0/b\bar{b}H^0$ vertex for H^0/h^0 production, respectively. We will not address this issue, which is part of a two-loop calculation, in this work. Therefore, we truncate Fig. 2 at $M_{A^0} = 150$ GeV.

For very large M_{A^0} the relative corrections to h^0 production increase to up to 10%. However, in this parameter region, the size of δ_{MSSM} for h^0 depends very sensitively on the definition of the effective mixing angle α_{eff} employed in σ_{IBA} . As defined in (2.52), α_{eff} inherits a distinct dependence on M_{A^0} because some of the self-energies are evaluated at momentum scales of the order of $M_{H^0} \sim M_{A^0}$. This dependence is not present in the complete result and, thus, has to be compensated by δ_{MSSM} . Evaluating the self-energies that enter α_{eff} (2.52) at $p^2 = 0$, the peak structure for large M_{A^0} in Fig. 2 is absent, and the size of the correction is 2–3% for $300 \text{ GeV} \lesssim M_{A^0} \lesssim 1000 \text{ GeV}$, as shown in Fig. 3. However, this approximation breaks down at small values of M_{A^0} where the corrections due to Higgs mixing become large. Note that in any case h^0 is SM-like at large M_{A^0} so that h^0 production is most likely of no phenomenological relevance.

The two-loop improvement of the self-energies of the CP-even Higgs bosons, as contained in the Z factors of (2.41) and (2.42), has a negligible effect on δ_{MSSM} for H^0 and A^0 production. Only for h^0 production and $M_{A^0} \lesssim 350$ GeV the difference between a one-loop and two-loop treatment is larger than 1% and can reach the 5% level for $M_{A^0} \approx 200$ GeV. However, the two-loop improvement plays an important role for the precise determination of the Higgs-boson pole masses entering the kinematics of the process [40].

It is important to emphasize that the size of the non-universal MSSM one-loop corrections δ_{MSSM} at large t_β is quite sensitive to the choice of the bottom-mass input value. This is caused by terms that grow as $m_b^2 t_\beta^2$ but are not included in the summation of t_β -enhanced terms. For the SPS 4 scenario, the b-mass input sensitivity is shown in Fig. 4. In the $\overline{\text{DR}}$ scheme for t_β (upper panel of Fig. 4) the absolute size of the non-universal corrections varies between approximately zero and -6% for H^0/A^0 production, depending on whether a massless approximation, the running mass or the pole mass is chosen as b-mass input. The sensitivity is even larger for the light Higgs h^0 . However, for h^0 production δ_{MSSM} depends very sensitively on the definition of α_{eff} , as mentioned before. Although we assume that the running mass including the summation of t_β -enhanced terms is a sensible choice, the sensitivity of the NLO correction to the b-mass input constitutes a theoretical uncertainty which can not be resolved at the NLO level.

Comparing the $\overline{\text{DR}}$ and the DCPR schemes for the renormalization of t_β , the size of the corrections is accidentally very similar if the running b-mass is chosen as an input. The same observation holds for the Higgs masses, which differ by less than 500 MeV. However, because of the large m_b dependence the corrections in the different renormalization schemes can differ significantly in general. This can be seen by comparing the upper and lower panels of Fig. 4. For the Higgs masses we also find larger differences up to 4 GeV for $m_b = 4.2$ GeV. Of course, the large scheme difference of the relative correction is partially compensated by the corresponding change in the DCPR input value for t_β to be calculated from the $\overline{\text{DR}}$ value $t_\beta = 50$. In the massless-b approximation, we find $t_\beta = 51.78$, while $t_\beta = 47.00$ for $m_b = 4.2$ GeV. The resulting scheme dependence of the total cross-section prediction for H^0 and A^0 production is thus moderate (below 1%) even for large m_b . For h^0 and large m_b , the residual scheme dependence can reach up to 3%. To compare the cross sections, we have used the on-shell mass for A^0 as computed in the $\overline{\text{DR}}$ scheme as input in both schemes.

We have verified that the size of δ_{MSSM} for H^0 or A^0 production does not change significantly when the input values of the soft breaking parameters for the sfermions or the soft breaking parameters for the gauginos are varied around their SPS 4 values by up to a factor of 2, unless some sparticles become unreasonably light.

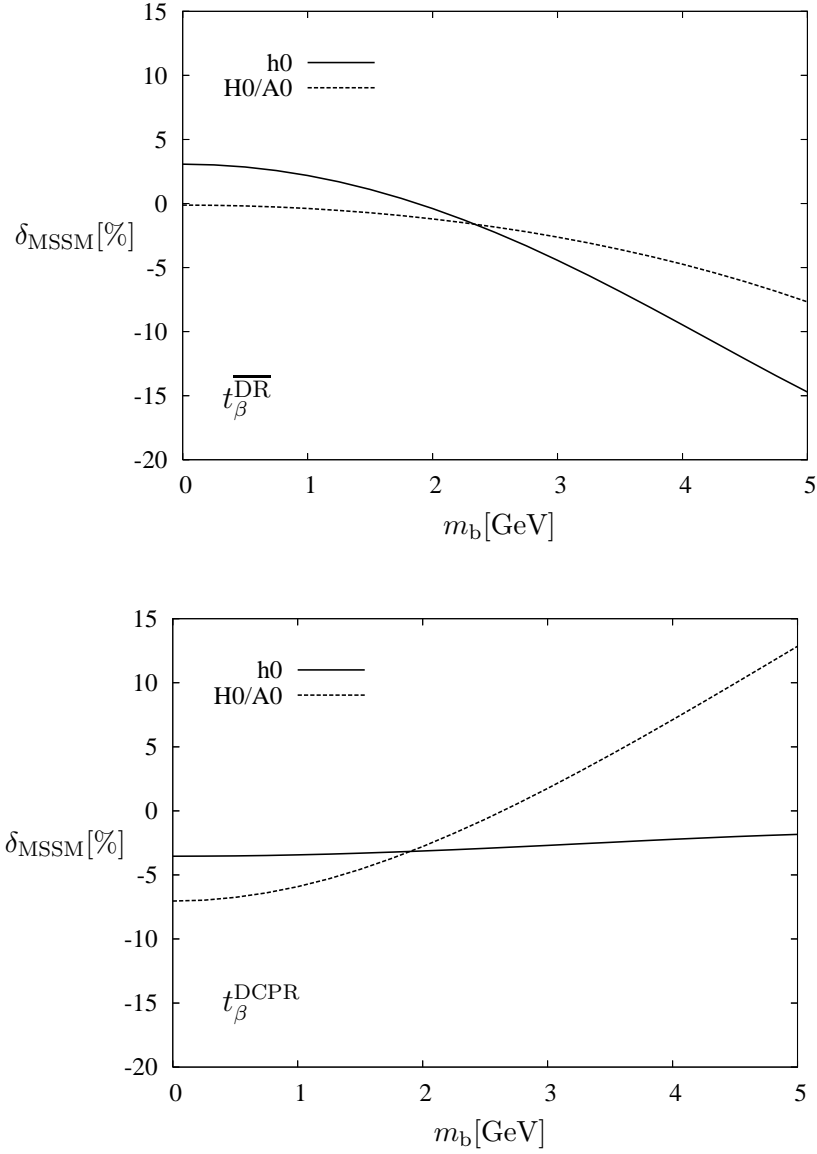


Figure 4: Full MSSM corrections $\delta_{\text{MSSM}} = \delta_{\text{MSSM-QCD}} + \delta_{\text{MSSM-weak}}$ defined relative to σ_{IBA} as a function of the m_b input in the $\overline{\text{DR}}$ scheme (upper panel) and DCPR scheme (lower panel) for t_β . The corrections for H^0 and A^0 lie on top of each other.

Results for the alternative benchmark scenario SPS 1b with $t_\beta = 30$ are presented in Appendix B. The conclusions reached for the SPS 4 scenario essentially hold for SPS 1b as well.

4 Conclusions

We have performed a complete calculation of the $\mathcal{O}(\alpha_s)$ and $\mathcal{O}(\alpha)$ corrections to associated bottom–Higgs production through $b\bar{b}$ fusion in the MSSM. This next-to-leading order prediction is improved by including two-loop corrections, as provided by `FeynHiggs`, and by the known summation of t_β -enhanced corrections. We have presented details of the calculation and discussed numerical results for MSSM Higgs-boson production at the LHC in two supersymmetric scenarios. The leading supersymmetric higher-order corrections, in particular the t_β -enhanced contributions, can be taken into account by an appropriate definition of the couplings and the running b-mass in an improved Born approximation. The remaining non-universal corrections are small, typically of the order of a few percent. The quality of an improved Born approximation, however, can only be judged with a full $\mathcal{O}(\alpha_s)$ and $\mathcal{O}(\alpha)$ calculation. Although we assume that the running mass including the summation of t_β -enhanced terms is a sensible choice for the input b-mass, alternative choices can lead to non-universal corrections as large as 10%.

With the results presented, the impact of the complete MSSM corrections to neutral Higgs boson decays into bottom quarks might also be updated.

Our results show that the difference between a properly defined improved Born approximation and the complete NLO calculation, which is improved by leading NNLO effects, is smaller than other theoretical uncertainties resulting from residual scale dependences, errors on the b-quark mass, and parton distribution functions.

Acknowledgments

We are grateful to Sven Heinemeyer, Wolfgang Hollik, and Georg Weiglein for discussions and comments on the manuscript.

A SPS benchmark scenarios

For the SPS benchmark [38] scenarios discussed in this work we use the following input for t_β , the mass of the CP-odd Higgs boson M_{A^0} , the supersymmetric Higgs mass parameter μ , the electroweak gaugino mass parameters $M_{1,2}$, the gluino mass $m_{\tilde{g}}$, the trilinear couplings $A_{\tau,t,b}$, the scale, at which the $\overline{\text{DR}}$ input values are defined $\mu_R(\overline{\text{DR}})$, the soft SUSY-breaking parameters in the diagonal entries of the squark and slepton mass matrices of the first and second generation M_{fi} (where $i = L, R$ refers to the left- and right-handed sfermions, $f = q, l$ to quarks and leptons, and $f = u, d, e$ to up and down quarks and electrons, respectively), and the analogous soft SUSY-breaking parameters for the third generation M_{fi}^{3G} :

	SPS 4	SPS 1b		SPS 4	SPS 1b
t_β	50.0	30.0	$M_{qL}[\text{GeV}]$	732.2	836.2
$M_{A^0}[\text{GeV}]$	404.4	525.5	$M_{dR}[\text{GeV}]$	713.9	803.9
$\mu[\text{GeV}]$	377.0	495.6	$M_{uR}[\text{GeV}]$	716.0	807.5
$M_1[\text{GeV}]$	120.8	162.8	$M_{lL}[\text{GeV}]$	445.9	334.0
$M_2[\text{GeV}]$	233.2	310.9	$M_{eR}[\text{GeV}]$	414.2	248.3
$m_{\tilde{g}}[\text{GeV}]$	721.0	916.1	$M_{qL}^{3G}[\text{GeV}]$	640.1	762.5
$A_\tau[\text{GeV}]$	-102.3	-195.8	$M_{dR}^{3G}[\text{GeV}]$	673.4	780.3
$A_t[\text{GeV}]$	-552.2	-729.3	$M_{uR}^{3G}[\text{GeV}]$	556.8	670.7
$A_b[\text{GeV}]$	-729.5	-987.4	$M_{lL}^{3G}[\text{GeV}]$	394.7	323.8
$\mu_R(\overline{\text{DR}})[\text{GeV}]$	571.3	706.9	$M_{eR}^{3G}[\text{GeV}]$	289.5	218.6

B Results for SPS 1b

In the SPS 1b scenario the two-loop Higgs masses are given by $M_{h^0} = 117.67$ GeV, $M_{H^0} = 525.69$ GeV, and $M_{A^0} = 525.66$ GeV in the $\overline{\text{DR}}$ scheme for t_β . Here, the masses in the DCPR scheme also differ by not more than 500 MeV and the discrepancy does not increase as drastically as in SPS 4 when the input value for the b-mass is changed with respect to its default value $m_b = 2.30$ GeV. As can be seen from Table 4, the non-universal corrections in the MSSM for A^0/H^0 -production are even smaller than for SPS 4. Because the masses of A^0/H^0 are larger and $t_\beta = 30$ is smaller than in SPS 4, the total production cross sections are also smaller. The cross sections including the cumulating effect of the different higher-order corrections are shown in Table 5. The generic structure of δ_{MSSM} as a function of M_{A^0} with all other SPS 1b parameters fixed, Fig. 5, does not differ from SPS 4.

	h^0	H^0	A^0
$\sigma_{\text{IBA}}[\text{pb}]$	0.59	1.88	1.88
$\delta_{\text{QCD}}[\%]$	35.98	19.02	19.02
$\delta_{\text{QED}}[\%]$	-0.13	-0.26	-0.26
$\delta_{\text{MSSM-QCD}}[\%]$	-0.06	0.11	0.11
$\delta_{\text{MSSM-weak}}[\%]$	2.73	-0.35	-0.35

Table 4: LO cross section in the improved Born approximation σ_{IBA} as defined in (2.53), as well as corrections δ relative to σ_{IBA} , for $pp \rightarrow (b\bar{b}) h^0/H^0/A^0 + X$ at the LHC ($\sqrt{s} = 14$ TeV) in the SPS 1b scenario. See Table 2 for details.

	h ⁰		H ⁰		A ⁰	
	m _b [GeV]	σ[pb]	m _b [GeV]	σ[pb]	m _b [GeV]	σ[pb]
QCD	2.79	0.85	2.50	2.64	2.50	2.64
+QED	2.79	0.84	2.50	2.63	2.50	2.63
+Δ _b ^{\tilde{g}}	2.76	0.83	2.08	1.82	2.08	1.82
+Δ _b ^{weak}	2.77	0.83	2.30	2.24	2.30	2.24
+sin(α _{eff})	2.77	0.80	2.30	2.24	2.30	2.24
full calculation	2.77	0.81	2.30	2.23	2.30	2.23

Table 5: The NLO MSSM cross section $pp \rightarrow (b\bar{b}) h^0/H^0/A^0 + X$ at the LHC ($\sqrt{s} = 14$ TeV) in the SPS 1b scenario. See Table 3 for details.

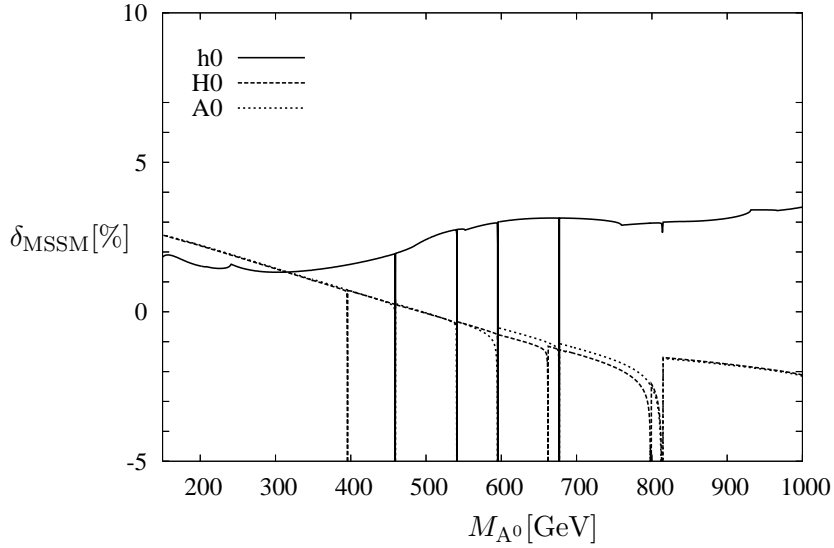


Figure 5: Full MSSM corrections $\delta_{\text{MSSM}} = \delta_{\text{MSSM-QCD}} + \delta_{\text{MSSM-weak}}$ defined relative to σ_{IBA} as a function of the M_{A^0} pole mass in the $\overline{\text{DR}}$ scheme for t_β . All other MSSM parameters are fixed to their SPS 1b values.

References

- [1] R. Raitio and W. W. Wada, Phys. Rev. D **19** (1979) 941;
J. N. Ng and P. Zakarauskas, Phys. Rev. D **29** (1984) 876;
Z. Kunszt, Nucl. Phys. B **247**, 339 (1984).
- [2] A. Abulencia *et al.* [CDF Collaboration], Phys. Rev. Lett. **96** (2006) 011802 [hep-ex/0508051];
V. M. Abazov *et al.* [D0 Collaboration], Phys. Rev. Lett. **97** (2006) 121802 [hep-ex/0605009].
- [3] M. Carena, S. Heinemeyer, C. E. M. Wagner and G. Weiglein, Eur. Phys. J. C **45** (2006) 797 [hep-ph/0511023].
- [4] R. M. Barnett, H. E. Haber and D. E. Soper, Nucl. Phys. B **306** (1988) 697;
D. A. Dicus and S. Willenbrock, Phys. Rev. D **39** (1989) 751.
- [5] S. Dittmaier, M. Krämer and M. Spira, Phys. Rev. D **70** (2004) 074010 [hep-ph/0309204].
- [6] J. Campbell *et al.*, [hep-ph/0405302].
- [7] S. Dawson, C. B. Jackson, L. Reina and D. Wackerroth, Mod. Phys. Lett. A **21** (2006) 89 [hep-ph/0508293].
- [8] C. Buttar *et al.*, [hep-ph/0604120].
- [9] W. Hollik and M. Rauch, [hep-ph/0610340];
G. Gao, R. J. Oakes and J. M. Yang, Phys. Rev. D **71** (2005) 095005, [hep-ph/0412356].
- [10] D. Dicus, T. Stelzer, Z. Sullivan and S. Willenbrock, Phys. Rev. D **59** (1999) 094016 [hep-ph/9811492].
- [11] R. V. Harlander and W. B. Kilgore, Phys. Rev. D **68** (2003) 013001 [hep-ph/0304035].
- [12] A. Dabelstein, Nucl. Phys. B **456** (1995) 25 [hep-ph/9503443].
- [13] T. Hahn, S. Heinemeyer, F. Maltoni, G. Weiglein and S. Willenbrock, [hep-ph/0607308].
- [14] H. E. Haber and G. L. Kane, Phys. Rept. **117** (1985) 75;
J. F. Gunion and H. E. Haber, Nucl. Phys. B **272** (1986) 1 [Erratum-ibid. B **402** (1993) 567].
- [15] E. Braaten and J. P. Leveille, Phys. Rev. D **22** (1980) 715;
M. Drees and K. I. Hikasa, Phys. Lett. B **240** (1990) 455 [Erratum-ibid. B **262** (1991) 497].
- [16] L. J. Hall, R. Rattazzi and U. Sarid, Phys. Rev. D **50** (1994) 7048 [hep-ph/9306309].
- [17] R. Hempfling, Phys. Rev. D **49** (1994) 6168.
- [18] M. Carena, M. Olechowski, S. Pokorski and C. E. M. Wagner, Nucl. Phys. B **426** (1994) 269 [hep-ph/9402253].
- [19] D. M. Pierce, J. A. Bagger, K. T. Matchev and R. J. Zhang, Nucl. Phys. B **491** (1997) 3 [hep-ph/9606211].

- [20] M. Carena, D. Garcia, U. Nierste and C. E. M. Wagner, Nucl. Phys. B **577** (2000) 88 [hep-ph/9912516].
- [21] J. Guasch, P. Häfliger and M. Spira, Phys. Rev. D **68** (2003) 115001 [hep-ph/0305101].
- [22] K. P. Diener, S. Dittmaier and W. Hollik, Phys. Rev. D **72** (2005) 093002 [hep-ph/0509084].
- [23] A. D. Martin, R. G. Roberts, W. J. Stirling and R. S. Thorne, Eur. Phys. J. C **39** (2005) 155 [hep-ph/0411040].
- [24] S. Dittmaier, Nucl. Phys. B **565** (2000) 69 [hep-ph/9904440].
- [25] T. Hahn, Comput. Phys. Commun. **140** (2001) 418 [hep-ph/0012260];
T. Hahn and C. Schappacher, Comput. Phys. Commun. **143** (2002) 54 [hep-ph/0105349].
- [26] T. Hahn and M. Perez-Victoria, Comput. Phys. Commun. **118** (1999) 153 [hep-ph/9807565].
- [27] A. Dabelstein, Z. Phys. C **67** (1995) 495 [hep-ph/9409375].
- [28] A. Denner, Fortsch. Phys. **41** (1993) 307.
- [29] H. Burkhardt and B. Pietrzyk, Phys. Lett. B **356** (1995) 398;
S. Eidelman and F. Jegerlehner, Z. Phys. C **67** (1995) 585 [hep-ph/9502298].
- [30] A. Sirlin, Phys. Rev. D **22** (1980) 971;
W. J. Marciano and A. Sirlin, Phys. Rev. D **22** (1980) 2695 [Erratum-ibid. D **31** (1985) 213]
and Nucl. Phys. B **189** (1981) 442.
- [31] P. H. Chankowski, A. Dabelstein, W. Hollik, W. M. Mösle, S. Pokorski and J. Rosiek, Nucl. Phys. B **417** (1994) 101.
- [32] P. H. Chankowski, S. Pokorski and J. Rosiek, Nucl. Phys. B **423** (1994) 437 [hep-ph/9303309].
- [33] J. A. Aguilar-Saavedra *et al.*, Eur. Phys. J. C **46** (2006) 43 [hep-ph/0511344].
- [34] S. Heinemeyer, W. Hollik and G. Weiglein, Eur. Phys. J. C **16** (2000) 139 [hep-ph/0003022].
- [35] S. Heinemeyer, W. Hollik and G. Weiglein, Comput. Phys. Commun. **124** (2000) 76 [hep-ph/9812320];
S. Heinemeyer, W. Hollik and G. Weiglein, Eur. Phys. J. C **9** (1999) 343 [hep-ph/9812472];
T. Hahn, S. Heinemeyer, W. Hollik, G. Weiglein, Proceedings of the 2005 International Linear Collider Workshop (LCWS 2005), Stanford, California [hep-ph/0507009].
- [36] W. M. Yao *et al.* [Particle Data Group], J. Phys. G **33** (2006) 1.
- [37] F. Jegerlehner, J. Phys. G **29** (2003) 101 [hep-ph/0104304].
- [38] B. C. Allanach *et al.*, Eur. Phys. J. C **25** (2002) 113 [eConf **C010630** (2001) P125] [hep-ph/0202233].
- [39] T. Bhattacharya and S. Willenbrock, Phys. Rev. D **47** (1993) 4022;
B. A. Kniehl, C. P. Palisoc and A. Sirlin, Phys. Rev. D **66** (2002) 057902 [hep-ph/0205304].
- [40] G. Degrandi, S. Heinemeyer, W. Hollik, P. Slavich and G. Weiglein, Eur. Phys. J. C **28** (2003) 133 [hep-ph/0212020].